

# Dominant climatic factors driving annual runoff changes at the catchment scale across China

Zhongwei Huang<sup>1, 2, 3</sup>, Hanbo Yang<sup>1\*</sup> and Dawen Yang<sup>1</sup>

[1]{State Key Laboratory of Hydro-Science and Engineering, Department of Hydraulic Engineering, Tsinghua University, Beijing, 100084, China}

[2]{Key Laboratory of Water Cycle and Related Land Surface Processes, Institute of Geographic Sciences and Natural Resources Research, Chinese Academy of Sciences, Beijing 100101, China}

[3]{University of Chinese Academy of Sciences, Beijing 100049, China}

Correspondence to: Hanbo Yang (yanghanbo@tsinghua.edu.cn)

## Abstract

With global climate changes intensifying, the hydrological response to climate changes has attracted more attention. It is beneficial not only for hydrology and ecology but also for water resource planning and management to understand the impact of climate change on runoff. In addition, there are large spatial variations in climate type and geographic characteristics across China. To gain a better understanding of the spatial variation of the response of runoff to changes in climatic factors and to detect the dominant climatic factors driving changes in annual runoff, we chose the climate elasticity method proposed by Yang and Yang (2011). It is shown that, in most catchments of China, increasing air temperature and relative humidity have negative impacts on runoff, while declining net radiation and wind speed have positive impacts on runoff, which slow the overall decline in runoff. Regarding the dominant climatic factor driving annual runoff, it is precipitation in most parts of China; net radiation mainly in some catchments of southern China; air temperature and wind speed mainly in some catchments of northern China.

## 1 Introduction

Climate change has become increasingly significant, and it has important impacts on the hydrological cycle and water resource management. Changes in climatic factors and runoff have been observed in many different regions of China. Reductions in precipitation occurred in the Hai River basin, the upper reaches of the Yangtze River basin and the Yellow River basin, and an increase occurred in western China (Yang et al., 2014a). A 29% decline in surface wind speed occurred in China during 1966 to 2011 (Liu et al., 2014). Most of the river basins in north China have exhibited an obvious decline in mean annual runoff, such as the Shiyang River basin (Ma et al., 2008), the Yellow River basin (Yang et al., 2004; Tang et al., 2007; Cong et al., 2009), and the Hai River basin (Ma et al., 2010). The hydrologic processes have been influenced by different climatic factors. For example, a decline in land surface wind speed can lead to a decrease in evapotranspiration, and changes in precipitation may affect water generation and concentration. However, the dominant climatic factor driving annual runoff change is still unknown in many catchments in China.

There are several approaches to investigate the impacts of annual runoff on climate change, including hydrologic models (Yang et al., 1998; Arnold et al., 1998; Yang et al., 2000; Arnold and Fohrer, 2005), the climate elasticity method (Schaake, 1990; Sankarasubramanian et al., 2001) and the statistics method (Vogel et al., 1999). The climate elasticity method, which has the advantage of requiring only the mean and trend of climate and basin variables and not requiring extensive historical measurements, was widely used in quantifying the effects of climatic factors on runoff, such as in the Yellow River basin (Zheng et al., 2009; Yang and Yang, 2011), the Luan River basin (Xu et al., 2013), the Chao-Bai Rivers basin (Ma et al., 2010), and the Hai River basin (Ma et al., 2008; Yang and Yang, 2011).

A simple climate elasticity method was first defined by Schaake (1990) to estimate the impacts of precipitation ( $P$ ) on annual runoff ( $R$ ):

$$\frac{dR}{R} = \varepsilon_p(P, R) \frac{dP}{P}, \quad (1)$$

where  $\varepsilon_p$  is the precipitation elasticity. To consider the effects of precipitation and air temperature on runoff, Fu et al. (2007) calculated the runoff change as:

$$\frac{dR}{R} = \varepsilon_a \frac{dP}{P} + \varepsilon_b \frac{dT}{T}, \quad (2)$$

where  $\varepsilon_a$  and  $\varepsilon_b$  are the precipitation elasticity and air temperature elasticity, respectively.

Five categories of methods can be used to estimate climate elasticity (Sankarasubramanian et al., 2001). The analytical derivation method has been widely used in many studies because it is clear in theory and does not need a large amount of historical observed data. Arora (2002) proposed an equation to calculate the response of runoff to precipitation and potential evaporation:

$$\frac{\Delta R}{R} = \left[1 + \frac{\phi F'_0(\phi)}{1 - F_0(\phi)}\right] \frac{\Delta P}{P} - \frac{\phi F'_0(\phi)}{1 - F_0(\phi)} \frac{\Delta E}{E}, \quad (3)$$

where  $\phi = E/P$  and  $F_0(\phi)$  is a Budyko formula and  $F'_0(\phi)$  is the derivation of  $\phi$ . The climate elasticity of runoff was evaluated in the upper reaches of the Yellow River basin by using Eq. (3) (Zheng et al., 2009). To evaluate the impacts from other climatic factors, Yang and Yang (2011) proposed an analytical method, based on the Penman equation and the annual water balance equation, to quantify the runoff change relative to changes in different climatic factors. By taking advantage of the mean annual climatic factors in the study period, the runoff elasticity to precipitation ( $P$ ), mean air temperature ( $T$ ), net radiation ( $R_n$ ), relative humidity ( $RH$ ), and wind speed ( $U_2$ ) were derived. The runoff change can be expressed as follows:

$$\frac{dR}{R} = \varepsilon_P \frac{dP}{P} + \varepsilon_{R_n} \frac{dR_n}{R_n} + \varepsilon_T dT + \varepsilon_{U_2} \frac{dU_2}{U_2} + \varepsilon_{RH} \frac{dRH}{RH}, \quad (4)$$

where  $\varepsilon_P$ ,  $\varepsilon_{R_n}$ ,  $\varepsilon_T$ ,  $\varepsilon_{U_2}$ , and  $\varepsilon_{RH}$  are the runoff elasticity relative to precipitation ( $P$ ), net radiation ( $R_n$ ), mean air temperature ( $T$ ), wind speed ( $U_2$ ), and relative humidity ( $RH$ ), respectively. However, this method was only tested in several catchments of non-humid north China.

There are large spatial variations in both geographic characteristics and climate types across China, resulting in a large variation in the hydrologic response to climate change. Therefore, the current study aims to (1) further validate the method proposed by Yang and Yang (2011), (2) evaluate the climate elasticity of climatic factors to runoff at the catchment scale across China, and (3) estimate the contribution of climatic factors to runoff change and then detect the dominant climatic factor driving annual runoff change.

## 2 Climate elasticity method based on the Budyko hypothesis

At the catchment scale, there is a relationship of evaporation with available water and available energy, referred as the Budyko hypothesis (Budyko, 1961). Budyko defined the available energy as the water equivalent of net radiation  $R_n$  at a large spatial scale. However, at a small spatial scale, except for net radiation, the energy imported by horizontal advection will affect water and energy balances. The effects of the horizontal advection can be exposed by climatic factors, such as humidity and air temperature. At the same time, this effect of net radiation and these climatic factors can be estimated by potential evaporation. Therefore, Yang et al. (2008) chose potential evaporation to represent available energy and further derived an analytical equation of the Budyko hypothesis as follows:

$$E = \frac{E_0 P}{(P^n + E_0^n)^{1/n}}, \quad (5)$$

where the parameter  $n$  represents the characteristics of the catchment, such as land use and coverage change, vegetation, slopes and climate seasonality (Yang et al. 2014a). The water balance equation can be simplified as  $P = E + R$  at the catchment scale for a long term, so runoff can be expressed as follows:

$$R = P - \frac{E_0 P}{(E_0^n + P^n)^{1/n}}. \quad (6)$$

To attribute the contribution of changes in  $P$  and  $E_0$  to runoff, Yang and Yang (2011) derived a new equation:

$$\frac{dR}{R} = \varepsilon_1 \frac{dP}{P} + \varepsilon_2 \frac{dE_0}{E_0}, \quad (7)$$

where  $\varepsilon_1$  and  $\varepsilon_2$  are the climate elasticity of runoff relative to  $P$  and  $E_0$ , respectively; and

they can be estimated as  $\varepsilon_1 = \frac{(1 - \partial E / \partial P) P}{P - E}$  and  $\varepsilon_2 = -\frac{\partial E / \partial E_0 E_0}{P - E}$ . The potential evaporation  $E_0$  (mm day<sup>-1</sup>) can be evaluated by the Penman equation (Penman, 1948):

$$E_0 = \frac{\Delta}{\Delta + \gamma} (R_n - G) / \lambda + \frac{\gamma}{\Delta + \gamma} 6.43(1 + 0.536U_2)(1 - RH)e_s / \lambda, \quad (8)$$

and the physical meaning of these symbols are shown in Table 1.

Similar to Eq. (7), the response of potential evaporation to climatic factors can be estimated as:

$$\frac{dE_0}{E_0} = \varepsilon_3 \frac{dR_n}{R_n} + \varepsilon_4 dT + \varepsilon_5 \frac{dU_2}{U_2} + \varepsilon_6 \frac{dRH}{RH}, \quad (9)$$

where  $\varepsilon_3, \varepsilon_4, \varepsilon_5, \varepsilon_6$  are the elasticity of potential evaporation relative to net radiation, air

temperature, wind speed, and relative humidity, respectively. Therein,  $\varepsilon_3 = \frac{R_n}{E_0} \frac{\partial E_0}{\partial R_n}$ ,

$\varepsilon_4 = \frac{1}{E_0} \frac{\partial E_0}{\partial T}$ ,  $\varepsilon_5 = \frac{U_2}{E_0} \frac{\partial E_0}{\partial U_2}$ , and  $\varepsilon_6 = \frac{RH}{E_0} \frac{\partial E_0}{\partial RH}$ . Due to the complex relationship between

$E_0$  and  $T$ , the value of  $\frac{\partial E_0}{\partial T}$  was calculated by the finite difference method, while  $\frac{\partial E}{\partial P}$ ,  $\frac{\partial E}{\partial E_0}$ ,

$\frac{\partial E_0}{\partial R_n}$ ,  $\frac{\partial E_0}{\partial U_2}$  and  $\frac{\partial E_0}{\partial RH}$  were calculated by the finite differential method.

Yang and Yang (2011) substituted Eq. (9) into Eq. (7) and yielding the following:

$$\frac{dR}{R} = \varepsilon_1 \frac{dP}{P} + \varepsilon_2 \varepsilon_3 \frac{dR_n}{R_n} + \varepsilon_2 \varepsilon_4 dT + \varepsilon_2 \varepsilon_5 \frac{dU_2}{U_2} + \varepsilon_2 \varepsilon_6 \frac{dRH}{RH}. \quad (10)$$

Denoted Eq. (10) as follows:

$$R^* = P^* + R_n^* + T^* + U_2^* + RH^*, \quad (11)$$

where  $P^*, R_n^*, T^*, U_2^*$ , and  $RH^*$  symbolize the runoff changes caused by the changes in

$P, R_n, T, U_2$ , and  $RH$ , respectively. The largest one among them is considered as the dominant

climatic factor driving annual runoff change.

14

### 3 Data and method

#### 3.1 Study region and data

The catchment information data set was collected from the Ministry of Water Resources of

the People's Republic of China (Water Resources and Hydropower Planning and Design

General Institute, 2011). In the data set, the catchment boundary and runoff ratio were

available. Chinese water resources zoning was divided by level as follows: there are 10 first-

level basins, 80 second-level river basins and 210 third-level river basins (shown in Fig.1 (A)).

There are no observed meteorological data on Taiwan Island and no runoff in two inland

catchments in Xinjiang Province. Hence, 207 third-level catchments were selected in this study.

The meteorological data, obtained from 736 weather stations between 1961 and 2010 from the China Meteorological Administration (CMA), included precipitation, surface mean air temperature, maximum air temperature, minimum air temperature, relative humidity, sunshine hours, and wind speed. In addition, daily solar radiation during the period 1961–2010 was collected from 118 weather stations.

To obtain the annual climatic factors in each catchment, first, a 10 km grid covering the study area was prepared. Second, we interpolated the observed data of the meteorological stations into a grid. The interpolation method used for climatic factors was an inverse-distance weighted technique, except air temperature, which must consider the influence of elevation (Yang et al., 2006). Third, according to the 10 km grid data set, the average values of climatic factors of each catchment were calculated.

Because only 118 weather stations directly measured solar radiation, the daily net radiation  $R_n$  ( $\text{MJ m}^{-2} \text{ day}^{-1}$ ) was calculated by an empirical formulation (Allen et al., 1998):

$$R_n = (1 - \alpha_s) R_s - \sigma \left[ \frac{(T_{\max} + 273.15)^4 + (T_{\min} + 273.15)^4}{2} \right] \cdot \left( 0.1 + 0.9 \frac{n}{N} \right) \times (0.34 - 0.14 \sqrt{\frac{RH}{100}}) e_s \quad (12)$$

The physical meaning of these symbols are shown in Table 2.  $R_s$  was calculated by using the Angström formulation (Angström, 1924):

$$R_s = (a_s + b_s \times \frac{n}{N}) R_a, \quad (13)$$

where  $R_a$  is extra-terrestrial radiation; and  $a_s$  and  $b_s$  are parameters that were calibrated using the data at the 118 stations with solar radiation observations (Yang et al., 2006). In Eq. (12),  $e_s$  is estimated as:

$$e_s = 0.3054 \left[ \exp\left(\frac{17.27 T_{\max}}{T_{\max} + 237.3}\right) + \exp\left(\frac{17.27 T_{\min}}{T_{\min} + 237.3}\right) \right]. \quad (14)$$

The wind speed at the height of 2 m ( $U_2$ ,  $\text{m s}^{-1}$ ) was estimated from a logarithmic wind profile based on the observed wind speed at the height of 10 m (Allen et al., 1998):

$$U_2 = U_z \frac{4.87}{\ln(67.8z - 5.42)} = 0.75 U_{10}. \quad (15)$$

Based on Eq. (6), the runoff ratio ( $\alpha$ ) can be estimated as follows:

$$\alpha = \frac{R}{P} = 1 - \frac{E_0}{(E_0^n + P^n)^{1/n}}. \quad (16)$$

Furthermore, the catchment characteristics parameter  $n$  was calculated according to  $\alpha$ ,  $E_0$  and  $P$ .

### 3.2 Validation of the climate elasticity method

Two steps were taken for the validation of the climate elasticity method, namely validating Eq. (7) and validating Eq. (9).

A catchment in a humid region with observed data for annual precipitation, annual potential evaporation and annual runoff from 1956 to 2000 was chosen to validate Eq. (7), namely the Upper Bijiang River basin (shown in Fig. 1(B)). The Upper Bijiang River basin is located in the upper reaches of the Lancang River basin, with 495mm mean annual precipitation and 243mm mean annual runoff. The results given by Eq. (7) were compared with the observed results. This approach is reasonable because this catchment is located in the southwest mountainous region, where there is no remarkable impact from human activities. However, in most regions, both anthropogenic activities and climate change have become important factors driving runoff change, and observed runoff data include the effects not only from anthropogenic activities but also from climate change. Therefore, we additionally collected the modeled runoff change and the contribution from climate change for another two catchments from the literature, to validate the climate elasticity method, namely the Luan River basin and the Upper Hanjiang River basin (shown in Fig.1 (B)). The Luan River basin, located in North China, is a part of the Hai River basin. It has a mean annual precipitation of 455 mm, 75–85% of which falls from June to September. The Upper Hanjiang River basin, lying in the middle and lower reaches of the Yangtze River basin, finally flows into the Danjiangkou Reservoir. In the two catchments, runoff undergoes a remarkable change, and the causes for this runoff change were analyzed using hydrological models. Xu et al. (2013) assessed the response of annual runoff to anthropogenic activities and climate change in the Luan River basin by using the geomorphology-based hydrological model (GBHM). Sun et al. (2014) explored the contributions from climate change and variation of catchment properties variation to runoff change in the Upper Hanjiang River basin using three different methods: climate elasticity, decomposition, and dynamic hydrological modeling methods. To validate

the climate elasticity method, the results given by Eq. (7) were compared with the results in references Xu et al. (2013) and Sun et al. (2014).

Equation (9) is the first-order Taylor approximation of the Penman equation. We first evaluated the climate elasticity of potential evaporation relative to air temperature, net radiation, relative humidity, wind speed and the change in these climatic factors, and we further estimated the change in potential evaporation according to Eq. (9), denoted as  $E_0^*$ . On the other hand, we calculated the potential evaporation change ( $E_0^{**}$ ) as:

$$E_0^{**} = \frac{f(T + dT, R_n + dR_n, U_2 + dU_2, RH + dRH) - f(T, R_n, U_2, RH)}{E_0}, \quad (17)$$

where the function  $f()$  represents the Penman equation. Then, the first approximation  $E_0^*$  was compared with  $E_0^{**}$ , and the relative error was defined as follows:  $RE = (E_0^* - E_0^{**}) / E_0^{**}$ , which was an effective criterion to assess Eq.(9). In addition, the data of annual climatic factors in 207 catchments, which were interpolated from the meteorological station observations were used for validation.

### 3.3 Trend analysis

The Mann–Kendall (MK) nonparametric test (Kendall, 1948; Kendall, 1990) is an effective statistical tool for trend detection, especially for hydrological and meteorological time series (Maidment, 1993). The MK nonparametric test is widely used for its convenient calculation processes. The sample data are not necessary to obey some specific distribution, but they must be serially independent. In this study, we firstly evaluated the significance levels of the trend of the hydrological and meteorological time series which were set at 0.05 and 0.1, and then estimated the slope of the trend:

$$\beta = \text{median} \left[ \frac{(x_j - x_i)}{(j - i)} \right], \quad (18)$$

for all  $i < j$ ; where  $\beta$  is the magnitude of trend, and  $\beta > 0$  indicates an increasing trend, and  $\beta < 0$  indicates a decreasing trend.



## 4 Results

### 4.1 Validation of the climate elasticity method

Table 3 shows the comparisons of runoff change, which were assessed by the climate elasticity method, the hydrological models and the observed data. The runoff changes were 6.9% and 8.4% in the Upper Bijiang River basin, -21.4% and -30.8% in the Upper Luan River basin, 9.1% and -31.4% in the Lower Luan River basin, and -19.0% and -27.6% in the Upper Hanjiang River basin, as evaluated by the climate elasticity method and the observed data, respectively. The results evaluated by the climate elasticity method performed well in comparison with the observed data in these basins except for the Lower Luan River basin where anthropogenic heterogeneity, such as irrigation and reservoir operation, may be an important factor driving runoff change. Conversely, the climate contribution to runoff was -14% and -21.4% in the Upper Luan River basin, 12.4% and 9.1% in the Lower Luan River basin and -19.6% and -19.0% in the Upper Hanjiang River basin, as estimated by the climate elasticity method and the hydrological models, respectively. These results were as expected and may provide an effective assessment of runoff change without consideration of anthropogenic heterogeneity, making it possible to use the climate elasticity method to evaluate climate elasticity and the response of runoff to climate change both in humid and arid catchments.

Figure 2 (A) shows the relationship between the potential evaporation change evaluated by Eq. (9) and that evaluated by Eq. (17), with most of the points falling around the line  $y=x$ . The relative error (RE) (shown in Fig.2 (B)) mostly ranged from -3 to 1%. A high correlation and small relative errors show the accuracy of Eq. (9), making it possible to express potential evaporation change as a function of the variation of climatic factors.

### 4.2 The mean annual climatic factors

The mean annual precipitation, net radiation, air temperature, wind speed, and relative humidity for each catchment between 1961 and 2010 are shown in Fig.3. The mean annual precipitation in China, which had a typical spatial variation that decreased from the southeast to the northwest, ranged from 30 mm in the northwest inland to 1883 mm in the southeast coastal area. The net radiation differed from 3 to 10 ( $\text{MJ m}^{-2} \text{ d}^{-1}$ ) in China, of which the largest value occurred in the Qinghai-Tibet Plateau and the lowest value occurred in the

Sichuan Basin. The mean annual air temperature in China had a range of  $-3.3$ – $23.8$  °C, with a typical spatial variation of decreasing from the south to the north. The wind speed at a 2 m height in China ranged from 1 m/s to 4 m/s, with the highest value occurring in the north and the coastland and the lowest value occurring in the Sichuan Basin. The relative humidity, which ranged from 35% in the northwest to 82% in the southeast, had a positive correlation with the precipitation. According to Eq. (6), we can evaluate the mean annual runoff (shown in Fig. 3(F)). The annual mean runoff had a range of 0 mm to 1176 mm, exhibiting a similar spatial variation with that of precipitation.

#### 4.3 Climate elasticity of the 207 catchments

Figure 4 shows the climate elasticity of runoff to the climatic factors for each catchment. In the 207 catchments, precipitation elasticity  $\varepsilon_p$  ranged from 1.1 to 4.75 (2.0 on average), indicating that a 1% change in precipitation leads to a 1.1–4.75% change in runoff. The lowest value of  $\varepsilon_p$ , ranging from 1.1 to 1.5, occurred in southern China. The highest value of  $\varepsilon_p$  mostly occurred in the Huai River basin, the Liao River basin, and the Hai River basin, and the lower reaches of Yellow River basin, indicating the highest sensitivity of runoff to precipitation change in these regions.

A 1%  $R_n$  change may result in  $-2.1\%$ – $0\%$  ( $-0.5$  on average) runoff change. The high value of  $-2.1 < \varepsilon_{R_n} < -0.8$  mostly occurred in the Huai River basin, the Hai River basin, and the lower reaches of the Yellow River basin, while the relatively small value of  $-0.4 < \varepsilon_{R_n} < 0$  mostly occurred in southern and northwest China.

The air temperature elasticity, ranging from  $-0.002/^\circ\text{C}$  to  $-0.095/^\circ\text{C}$  ( $-0.025/^\circ\text{C}$  on average), indicates that a 1 centigrade degree increase in air temperature may result in a 0.2%–9.5% decrease in runoff. The high value of  $-0.095/^\circ\text{C} < \varepsilon_T < -0.026/^\circ\text{C}$  mainly occurred in the Songhua River basin, the Liao River basin, the Hai River basin, the lower reaches of the Yellow River basin and the east part of the northwest area; while a small value of  $-0.025/^\circ\text{C} < \varepsilon_T < -0.001/^\circ\text{C}$  mainly occurred in the south and west regions of China. The absolute value of air temperature elasticity was small when compared with other elasticities, the reason for which will be discussed in Appendix .

The value of  $\varepsilon_{U_2}$  ranged from  $-0.01$  to  $-0.94$  ( $-0.22$  on average). The high value of  $-0.95 < \varepsilon_{U_2} < -0.5$  mostly occurred in the Yellow River basin, the Huai River basin, the Hai River basin and the Liao River basin, indicating that a 1% wind speed decrease will lead to a 0.5% – 0.95% decline in runoff.

The value of  $\varepsilon_{RH}$  ranged from  $0.05$  to  $3$  ( $0.74$  on average), and the spatial distributions of these values were similar to those of precipitation.

#### 4.4 Changes in the climatic factors

Changes in climatic factors were shown in Fig.5. Significance and rate of changes in climatic factors from 1961 to 2010 have been reported by Yang et al. (2015). There is a large spatial variation in precipitation change which increased in the Northwest China (ranging from 5%/decade to 11%/decade,  $p < 0.05$ ) and decreased in the Yellow River basin, the Hai River basin and the upper reach of the Yangtze River basin (ranging from  $-5\%$ /decade to  $-2.5\%$ /decade,  $p < 0.05$ ), but there were no significant change trend shown in 130 catchments of the total 207 catchments.

Net radiation showed a decrease in most catchments. Large decrease (ranging from  $-6\%$ /decade to  $-3\%$ /decade) occurred in the Hai River basin, the Huai River basin and the lower reach of Yangtze River basin ( $p < 0.05$ ), while small decrease (ranging from  $-3\%$ /decade to  $-0\%$ /decade) occurred in the majority of the Northern China. No significant change trend was shown in the Qinghai-Tibet Plateau.

Air temperature increased all over the China. Large increase (ranging from  $0.4$  °C/decade to  $0.8$  °C/decade) mainly occurred in the Northern China ( $p < 0.05$ ), while small decrease (ranging from  $0$  to  $0.4$  °C/decade) occurred in the majority of the Southeast.

Wind speed decreased in most catchments, ranging from  $-11\%$ /decade in the southeast to  $-1\%$ /decade in the upper reach of Yangtze River basin. Only 5 catchment showed significant ( $p < 0.05$ ) increase in wind. Relative humidity increased in the western China (the maximum is about 3%/decade) and decreased in the Southeast China and the Yangtze River basin (ranging from  $-1.7\%$ /decade to  $-0.5\%$ /decade).

The change trend of relative humidity agreed with the change of precipitation, ranging from  $-1.7\%$ /decade in the east to  $3\%$ /decade in the west. Large increase (ranging from  $2\%$ /decade to  $3\%$ /decade) mainly occurred in the northwest China ( $p < 0.05$ ), while large decrease (ranging from  $-1.7\%$ /decade to  $-1\%$ /decade) main occurred in the middle reach of the Yellow River basin and the Songhua River basin ( $p < 0.05$ ).

#### **4.5 Contributions of climatic factors to runoff change**

Figure 6 shows the contributions of climatic factors to runoff change. The contribution of precipitation to the change of runoff has a distinct spatial variation. A positive contribution occurred in western China and southeast China, especially in the northwest China where the contribution of precipitation to runoff change ranges from  $12\%$ /decade to  $25\%$ /decade. A negative contribution mainly occurred in central and northeast China. In the middle reaches of the Yellow River basin and the Hai River basin, the negative contribution reached the highest, ranging from  $-18\%$ /decade to  $-10\%$ /decade.

A positive contribution of net radiation to runoff change occurred in most catchments, except for the Qinghai-Tibet Plateau. In the Hai River basin, the positive contribution reached the highest, ranging from  $3\%$ /decade to  $9\%$ /decade, compensating to some degree for the decline in runoff caused by precipitation decrease.

A negative contribution of air temperature to runoff change occurred in all of China. A large contribution ( $-1\%$  to  $-3\%$ /decade) mainly occurred in the Songhua River basin, the Liao River basin, the Hai River basin, the lower reaches of the Yellow River basin and the east part of northwest area; while a small contribution ( $0\%$  to  $-0.5\%$ /decade) mainly occurred in South China.

A positive contribution of wind speed to runoff change occurred in most catchments except for part of the upper reaches of Yangtze River basin. In the Hai River basin and the Liao River basin, the positive contribution reached the highest, ranging from  $2\%$ /decade to  $6\%$ /decade, compensating to some degree for the decline in runoff caused by precipitation decrease.

A negative contribution of relative humidity to runoff change occurred in most catchments except for part of northwest China where the positive contribution of relative humidity to the change of runoff ranges 0–2%/decade.

Figure 7 shows the dominant climatic factors driving runoff in the 207 catchments. In 143 of the total 207 catchments, the runoff change was dominated by precipitation. In addition, the runoff change was mainly determined by net radiation in some catchments of the lower reaches of the Yangtze River basin, the Pearl River basin, the Huai River basin and the southeast area; by air temperature in the upper reaches of the Yellow River basin and the north part of the Songhua River basin; and by wind speed in part of the northeast area, part of Inner Mongolia.

## **5 Discussion**

### **5.1 Climate elasticity**

The climate elasticity method was widely used to evaluate the hydrologic cycle in many catchments in China. Tables 4 and 5 show the comparison of our results with estimates of climate elasticities from various references, illustrating good agreement with our results in the same regions.

### **5.2 Effect of climate change on runoff**

The contribution of climatic factors to runoff change can be estimated by climate elasticity and changes in climatic factors.

The contribution of precipitation to runoff change has a regional pattern. A large negative contribution mainly occurred in the Hai River basin and the Yellow River basin, and the possible cause was the decrease in precipitation from 1961 to 2010. This decrease may be caused by weakening of the East Asian monsoon circulation (Xu et al., 2006). However, as a result of decreasing atmospheric stability and increasing amounts of transfer of water vapor, a significant increasing trend in precipitation occurred in Xinjiang Province and the Qinghai-Tibet Plateau (Bai and Xu, 2004), further leading to a positive contribution of precipitation to runoff change.

1 A large positive contribution of net radiation occurred in the Hai River basin and the Huai  
2 River basin, while a small contribution occurred in the Qinghai-Tibet Plateau. The main cause  
3 of these results was the spatial variation of the net radiation change. As a result of  
4 atmospheric dimming and the increase of atmospheric turbidity, there was an obvious  
5 decrease of the surface solar radiation in China, especially in the Hai River basin and the Huai  
6 River basin (Tang et al., 2011; Zhao et al., 2006). However, due to the thin and stable air  
7 condition, net radiation in Qinghai-Tibet Plateau changed little.

8 There was a significant warming trend for all of China during 1961–2010 due to human  
9 activities, including industrialization and agricultural production (Ren et al., 2012), leading to  
10 a negative contribution to runoff change. Remarkably, the climate elasticity method only  
11 analyzes the direct impact of air temperature on runoff, i.e., higher temperature leading to  
12 larger evaporative demand and further inducing more evaporation (less runoff). In fact, rising  
13 temperatures also have indirect impacts on runoff (Gardner, 2009). For example, Chiew et al.,  
14 (2009) reported that a degree global warming will result in –10 to 3% changes in precipitation  
15 in Australia, leading to runoff change. Furthermore, rising air temperatures will lead to a  
16 longer snowmelt period, further resulting in an increase in annual runoff (Li et al., 2013).

17 Due to the changes in atmospheric circulation and surface roughness, a weakening of wind  
18 speed has occurred in most regions of China, especially in eastern China where urbanization  
19 and environmental changes have taken place rapidly (Vautard et al., 2010; Hou et al., 2013).  
20 Consequently, the response of runoff to wind speed was intense in the Hai River basin, the  
21 Liao River basin and the northeast area, resulting in a large positive contribution of wind  
22 speed to runoff change.

23 A negative contribution of relative humidity to runoff change occurred in most regions in  
24 China, caused by the trend of relative humidity change. The annual relative humidity  
25 exhibited a reducing trend in most parts of China; one of the major causes for the reduction of  
26 relative humidity was that the increasing rates of specific humidity were smaller than those of  
27 surface saturation specific humidity with the increase of temperature (Song et al., 2012).

28 Precipitation is an important factor driving runoff change. Precipitation may directly impact  
29 the conditions of runoff yield or may affect the water supply conditions of evaporation and  
30 further affect runoff. Previous studies reported that precipitation decrease was the dominant  
31 factor of declining runoff in the Futuo River catchment (Yang and Yang, 2011) and the  
32 Yellow River basin (Tang et al., 2013), agreeing with our results.

1 In previous studies, when assessing the impacts of changes in climatic factors on runoff in  
2 China, wind speed declines were often identified as being important (Tang et al., 2011; Liu et  
3 al., 2014; McVicar et al., 2012). Wind speed decline tended to result in the decline of actual  
4 evapotranspiration and complementary increase of streamflow in wet river basins but had  
5 little impacts in dry basins (Liu et al., 2014), similar to our results. Remarkably, in some  
6 catchments of the northeast area and Inner Mongolia, declining wind speed had the greatest  
7 contribution to runoff change. In these catchments, changes in precipitation were minimal and  
8 the contribution of precipitation to runoff change was small compared with that of wind speed.

9 The runoff change was mainly determined by net radiation in some catchments of the lower  
10 reaches of the Yangtze River basin, the Pearl River basin, the Huai River basin and the  
11 southeast area, and by air temperature in the upper reaches of the Yellow River basin and the  
12 north part of the Songhua River basin. In these catchments, the precipitation elasticity was  
13 low; the changes were slight; and the contribution of precipitation to runoff was small.  
14 However, due to a significant decreasing trend in net radiation or obvious warming, changes  
15 in net radiation or air temperature had greater impacts on runoff compares with precipitation.

16 Remarkably, for a specific catchment, some climatic factors have a positive contribution to  
17 runoff, while others have a negative contribution. For example, in the Hai River basin,  
18 decreasing precipitation lead to  $-8\text{--}18\%$ /decade runoff change; at the same time, declining  
19 net radiation caused a  $2\text{--}9\%$ /decade runoff change, and weakening wind speed caused a  $1.5\text{--}$   
20  $4.5\%$ /decade runoff change, compensating for the runoff decline caused by decreasing  
21 precipitation. Consequently, the runoff decrease due to climate change is  $0\text{--}9\%$ /decade (Yang  
22 et al., 2014a). Conversely, in the middle reaches of the Yellow River basin, decreasing  
23 precipitation also has a  $-8\text{--}18\%$ /decade contribution to runoff, but the positive contributions  
24 from net radiation and wind speed are less than that in the Hai River basin, which leads to the  
25 largest runoff decline,  $5\text{--}13\%$ /decade in the Hai River basin (Yang et al., 2014a).

26 The dominant climatic factor driving runoff change was determined by the geographic  
27 conditions and climate change. In this study, we analyzed the contribution of climatic factors  
28 to runoff change by the climate elasticity method. This method only focused on the direct  
29 impact of climate change on runoff but ignored the interaction among the climatic factors.  
30 These interaction need further study.

### 5.3 Error analysis

In Eq. (10), the net radiation  $R_n$  and the air temperature  $T$  were considered as two independent variables. However, according to Eq. (12) and Eq. (13) the net radiation  $R_n$  is associated with the air temperature  $T$ . To verify the impact of the relationship between net radiation and air temperature on Eq. (12), the effect of the change in air temperature to change in net radiation  $R_n$  must be evaluated as follows:

$$dR_n = \frac{\Delta R_n}{\Delta T} dT . \quad (19)$$

If the effect of  $T$  on  $R_n$  is ignored, the relative error has been observed to be less than 1% ,as evaluated by Yang and Yang (2011) in the Futuo River basin.

In addition, Eq. (10) is a first-order approximation, probably resulting in errors in the estimating of climate elasticity. Yang et al. (2014a,b) evaluated that when the changes in potential evapotranspiration ( $\Delta E_0$ ) and precipitation ( $\Delta P$ ) are not large, the error of  $\varepsilon_p$  caused by first-order approximation can be neglected, but the error will increase with increasing changes, with a 0.5–5% relative error in  $\varepsilon_p$  when  $\Delta P = 10$  mm and a 5–50% relative error in  $\varepsilon_p$  when  $\Delta P = 100$  mm.

## 6 Conclusion

In this study, we used the climate elasticity method to reveal the dominant climatic factor driving annual runoff change across China. We first validated the climate elasticity method that was first derived by Yang and Yang (2011) . On account of China being a vast country with remarkable spatial differences in climate and geographical characteristics, we divided China into 207 catchments; evaluated the climate elasticity of runoff relative to precipitation, net radiation, air temperature, wind speed and relative humidity; and estimated the contribution of climatic factors to runoff change for each catchment.

In the 207 catchments, precipitation elasticity, which was low in southern China and part of the northwest area and high in the Liao River basin, the Hai River basin, and the Huai River basin, ranged from 1.1 to 4.8 (2.0 on average). This elasticity means that a 1% change in precipitation will lead to a 1.1%–4.8% change in runoff. The air temperature elasticity, which ranged from  $-0.002/^{\circ}\text{C}$  to  $-0.095/^{\circ}\text{C}$  ( $-0.025/^{\circ}\text{C}$  on average), net radiation elasticity, which



1 ranged from  $-0.1$  to  $-2$  ( $-0.5$  on average), wind speed elasticity, which ranged from  $-0.01$  to  
2  $0.94$  ( $-0.22$  on average) and relative humidity elasticity, which ranged from  $0.05$  to  $3$  ( $0.74$  on  
3 average), had similar distributions to precipitation elasticity.

4 A large negative contribution of precipitation to runoff change mainly occurred in the Hai  
5 River basin and the Yellow River basin, while a positive contribution occurred in Xinjiang  
6 Province and the Qinghai-Tibet Plateau. A large positive contribution of net radiation occurred  
7 in the Hai River basin and the Huai River basin, while a small contribution occurred in the  
8 Qinghai-Tibet Plateau. A negative contribution of air temperature to runoff change occurred  
9 in all of China. A positive contribution of wind speed to runoff change occurred in most parts  
10 of China, while a negative contribution of relative humidity to runoff change occurred in most  
11 regions of China. A  $5\text{--}13\%$ /decade decrease in runoff was caused by climate change in the  
12 middle reaches of the Yellow River basin and the Hai River basin (Yang et al., 2014a).  
13 Specifically, changes in precipitation, air temperature, and relative humidity contributed  
14 negative impacts on runoff. Simultaneously, declines in net radiation and wind speed had  
15 positive impacts on runoff, slowing the overall decline in runoff.

16 Precipitation was the dominant climatic factor driving runoff change in most of the 207  
17 catchments. Net radiation was dominant in some catchments of the lower reaches of the  
18 Yangtze River basin, the Pearl River basin, the Huai River basin and the southeast area; air  
19 temperature was dominant in the upper reaches of the Yellow River basin and the north part  
20 of the Songhua River basin; and wind speed in part of the northeast area, part of Inner  
21 Mongolia.

## 22 23 Appendix: The air temperature elasticity

24 The air temperature elasticity ranged from  $-0.002/^\circ\text{C}$  to  $-0.095/^\circ\text{C}$ , which was obviously  
25 smaller compared with other climatic elasticities. To explore the causes, air temperature  
26 elasticity was calculated by the following equation:

$$27 \quad \varepsilon_T = \varepsilon_2 \varepsilon_4 = \varepsilon_2 \frac{1}{E_0} \frac{\partial E_0}{\partial T} \Big|_{X=\bar{X}}, \quad (\text{A1})$$

28 where  $\varepsilon_2$  was the runoff elasticity to potential evaporation, ranging from  $-3$  to  $0$  in China.

29 Next, we will analyze the value of  $\frac{\partial E_0}{\partial T}$  by the differential method. Denoting Eq. (8) as

$E_0 = f_1(\Delta, e_s)$ , we can express  $\Delta$  ( $\text{kPa } ^\circ\text{C}^{-1}$ ) and  $e_s$  ( $\text{kPa}$ ) as  $\Delta = f_2(T)$  and  $e_s = f_3(T)$ , respectively. Due to their substitution,  $\frac{\partial E_0}{\partial T}$  can be expressed as:

$$\frac{\partial E_0}{\partial T} = \frac{\partial E_0}{\partial \Delta} \frac{\partial \Delta}{\partial T} + \frac{\partial E_0}{\partial e_s} \frac{\partial e_s}{\partial T}, \quad (\text{A2})$$

where 
$$\frac{\partial E_0}{\partial \Delta} = \frac{\gamma}{(\Delta + \gamma)^2} \left[ \frac{(R_n - G) - 6.43(1 + 0.536U_2)(1 - RH)e_s}{\lambda} \right] \quad \text{and}$$

$$\frac{\partial E_0}{\partial e_s} = \frac{\gamma}{\Delta + \gamma} 6.43(1 + 0.536U_2)(1 - RH) / \lambda.$$

Figure A1 shows the trend of  $\Delta$  and  $e_s$  as the change in temperature according to the relationship between  $\Delta$  and  $T$  and between  $e_s$  and  $T$ , where the average values of  $\frac{\partial \Delta}{\partial T}$  and  $\frac{\partial e_s}{\partial T}$  were 0.0047 and 0.08 in the 207 catchments, respectively.

Figure A2(A) and (B) show the relationship of  $\frac{\partial E_0}{\partial \Delta}$  and  $\frac{\partial E_0}{\partial e_s}$  with  $T$  in 207

basins of China.  $\frac{\partial E_0}{\partial \Delta}$  ranged from  $-5.5$  to  $9.3$  ( $0.22$  on average), while  $\frac{\partial E_0}{\partial e_s}$  which ranged

from  $0.3$  to  $1.9$  ( $0.85$  on average), decreased with rising air temperature. From the results above, it can be found that the absolute value of  $\frac{\partial E_0}{\partial \Delta} \frac{\partial \Delta}{\partial T}$  was small when compared with

$\frac{\partial E_0}{\partial e_s} \frac{\partial e_s}{\partial T}$  due to the small value of  $\frac{\partial \Delta}{\partial T}$ .  $\frac{\partial E_0}{\partial T}$  was mainly determined by  $\frac{\partial E_0}{\partial e_s}$ , indicating that

the rising air temperature mainly affected saturation vapor pressure, leading to changes in potential evaporation. Based on the results, Fig. A3 shows the relationship between  $T$  and

$\frac{\partial E_0}{\partial T}$  in 207 basins of China.  $\frac{\partial E_0}{\partial T}$  ranged from  $0.04$  to  $0.12$  in different basins, a decreasing

trend as  $T$  increased.

## Acknowledgements

This research was partially supported by funding from the National Natural Science Foundation of China (Nos.51379098 and 91225302) and the National Program for Support of

1 Top-notch Young Professionals. In addition, this research benefited from the China  
2 Meteorological Data Sharing Service System, which provided the meteorological data. We  
3 are grateful to the editor Hongyi Li and Maik Renner, Mishra Ashok and another anonymous  
4 referee for helpful comments.  
5

## 1   **References**

- 2   Allen, R., Pereira, L., Raes, D., and Smith, M.: Crop evapotranspiration: guidelines for  
3   computing crop water requirements. FAO Irrigation and Drainage Paper 56., Fao Irrigation &  
4   Drainage Paper, 1998.
- 5   Angström, A.: Solar and terrestrial radiation, Quarterly Journal of the Royal Meteorological  
6   Society, 50, 121-126, 1924.
- 7   Arnold, J. G., and Fohrer, N.: SWAT2000: current capabilities and research opportunities in  
8   applied watershed modelling, Hydrological Processes, 19, 563-572, 2005.
- 9   Arnold, J. G., Srinivasan, R., Muttiah, R. R., and Williams, J. R.: Large hydrologic modeling  
10   and assessment Part 1: Model development, J.am.water Resour.assoc, 34, 73–89, 1998.
- 11   Arora, V. K.: The use of the aridity index to assess climate change effect on annual runoff,  
12   Journal of Hydrology, 265, 164–177, 2002.
- 13   Bai, J., and Xu, X.: Atmospheric hydrological budget with its effects over Tibetan plateau,  
14   Journal of Geographical Sciences, 14, 81-86, 2004.
- 15   Budyko, M. I.: The Heat Balance of the Earth's Surface, Soviet Geography, 2, 3-13, 1961.
- 16   Chiew, F., Teng, J., Vaze, J., and Kirono, D.: Influence of global climate model selection on  
17   runoff impact assessment, Journal of Hydrology, 379, 172-180, 2009.
- 18   Cong, Z., Yang, D., Gao, B., Yang, H., and Hu, H.: Hydrological trend analysis in the Yellow  
19   River basin using a distributed hydrological model, Water Resources Research, 45, 335-345,  
20   2009.
- 21   Fu, G., Charles, S. P., and Chiew, F. H. S.: A two-parameter climate elasticity of streamflow  
22   index to assess climate change effects on annual streamflow, Water Resources Research, 43,  
23   W11419, 10.1029/2007WR005890, 2007.
- 24   Gardner, L. R.: Assessing the effect of climate change on mean annual runoff, Journal of  
25   Hydrology, 379, 351–359, 2009.
- 26   Hou, A., Ni, G., Yang, H., and Lei, Z.: Numerical analysis on the contribution of urbanization  
27   to wind stilling: an example over the Greater Beijing Metropolitan area, Journal of Applied  
28   Meteorology and Climatology, 52(5), 1105-1115.

1 Jiang, T., Chen, Y. D., Xu, C. Y., Chen, X., Chen, X., and Singh, V. P.: Comparison of  
2 hydrological impacts of climate change simulated by six hydrological models in the  
3 Dongjiang Basin, South China, *Journal of Hydrology*, 336, 316–333, 2007.

4 Kendall, M. G.: Rank correlation methods, *Biometrika*, 1948.

5 Kendall, M. G., J. D.: Rank Correlation Methods, Oxford University Press, Oxford, 1990.

6 Li, B. et al.: Variations of temperature and precipitation of snowmelt period and its effect on  
7 runoff in the mountainous areas of Northwest China, *Journal of Geographical Sciences*, 23,  
8 17-30, 2013.

9 Liu, X., Zhang, X. J., Tang, Q., and Zhang, X. Z.: Effects of surface wind speed decline on  
10 modeled hydrological conditions in China, *Hydrology & Earth System Sciences*, 18, 2803-  
11 2813, 2014.

12 Ma, H., Yang, D., Tan, S. K., Gao, B., and Hu, Q.: Impact of climate variability and human  
13 activity on streamflow decrease in the Miyun Reservoir catchment, *Journal of Hydrology*, 389,  
14 317-324, 2010.

15 Ma, Z., Kang, S., Zhang, L., Tong, L., and Su, X.: Analysis of impacts of climate variability  
16 and human activity on streamflow for a river basin in arid region of Northwest China, *Journal*  
17 *of Hydrology*, 352, 239-- 249, 2008.

18 Mainment, D. R.: Handbook of Hydrology, McGraw-Hill, New York, 1993.

19 Mcvicar, T. R., Roderick, M. L., Donohue, R. J., and Van Niel, T. G.: Less bluster ahead?  
20 Ecohydrological implications of global trends of terrestrial near-surface wind speeds,  
21 *Ecohydrology*, 5, 381–388, 2012.

22 Penman, H. L.: Natural evaporation from open water, Bare Soil and Grass, Royal Society of  
23 London Proceedings, 193, 120-145, 1948.

24 Ren, G., Ding, Y., Zhao, Z., Zheng, J., Wu, T., Tang, G. and Xu, Y.: Recent progress in  
25 studies of climate change in China, *Adv Atmos Sci*, 29, 958–977, 2012.

26 Sankarasubramanian, A., Vogel, R. M., and Limbrunner, J. F.: Climate elasticity of  
27 streamflow in the United States, *Water Resources Research*, 37, 1771–1781, 2001.

28 Schaake, J. C.: From climate to flow, *Climate change and US water resources.*, edited by:  
29 Waggoner, P. E., John Wiley, New York, 177-206 pp., 1990.

- 1 Song, Y., Liu, Y., and Ding, Y.: A study of surface humidity changes in china during the  
2 recent 50 years, *Acta Meteorologica Sinica*, 26, 541-553, 2012.
- 3 Sun, S., Chen, H., Ju, W., Song, J., Zhang, H., Sun, J., and Fang, Y.: Effects of climate  
4 change on annual streamflow using climate elasticity in Poyang Lake Basin, China,  
5 *Theoretical & Applied Climatology*, 112, 169-183, 2013.
- 6 Sun, Y., Tian, F., Yang, L., and Hu, H.: Exploring the spatial variability of contributions from  
7 climate variation and change in catchment properties to streamflow decrease in a mesoscale  
8 basin by three different methods, *Journal of Hydrology*, 508, 170–180, 2014.
- 9 Tang, B., Tong, L., Kang, S., and Zhang, L.: Impacts of climate variability on reference  
10 evapotranspiration over 58 years in the Haihe river basin of north China, *Agricultural Water  
11 Management*, 98, 2011.
- 12 Tang, Q., Oki, T., Kanae, S., and Hu, H.: The influence of precipitation variability and partial  
13 irrigation within grid cells on a hydrological simulation, *Journal of Hydrometeorology*, 8, 499,  
14 2007.
- 15 Tang, W., Yang, K., Qin, J., Cheng, C. and He, J.: Solar radiation trend across China in recent  
16 decades: a revisit with quality-controlled data, *Atmos Chem Phys*, 11, 393–406, 2011.
- 17 Tang, Y., Tang, Q., Tian, F., Zhang, Z., and Liu, G.: Responses of natural runoff to recent  
18 climatic variations in the Yellow River basin, China, *Hydrology & Earth System Sciences*, 17,  
19 4471-4480, 2013.
- 20 Vautard, R., Cattiaux, J., Yiou, P., Thepaut, J. and Ciais, P.: Northern Hemisphere  
21 atmospheric stilling partly attributed to an increase in surface roughness, *Nat Geosci*, 3:756–  
22 761,2010.
- 23 Vogel, R. M., Wilson, I., and Daly, C.: Regional regression models of annual streamflow for  
24 The United States, *Journal of Irrigation & Drainage Engineering*, 125, 148-157, 1999.
- 25 Wang, Z., Shen, Y., and Song, L.: Hydrologic response of the climatic change based on  
26 SWAT Model in Beijiing River basin, *Meteorological & Environmental Research*, 8-12, 2013.
- 27 Water Resources and Hydropower Planning and Design General Institute, Specification for  
28 Comprehensive Water Resources Zoning, China Water & Power Press, Beijing China, 2011.

1 Xu, M., Chang, C., Fu, C., Qi, Y., Robock, A., Robinson, D. and Zhang, H.: Steady decline of  
2 east Asian monsoon winds, 1969–2000: evidence from direct ground measurements of wind  
3 speed, *J Geophys Res*, 111:D24, 2006.

4 Xu, X., Yang, H., Yang, D., and Ma, H.: Assessing the impacts of climate variability and  
5 human activities on annual runoff in the Luan River basin, China, *Hydrology Research*, 44,  
6 940-952, 2013.

7 Yang, D., Herath, S., and Musiake, K.: Development of geomorphology-based hydrological  
8 model for large catchments, *Proceedings of Hydraulic Engineering*, 42, 169-174, 1998.

9 Yang, D., Herath, S., and Musiake, K.: Comparison of different distributed hydrological  
10 models for characterization of catchment spatial variability, *Hydrological Processes*, 14, 403-  
11 416, 2000.

12 Yang, D., Li, C., Hu, H., Lei, Z., Yang, S., Kusuda, T., Koike, T., and Musiake, K.: Analysis  
13 of water resources variability in the Yellow River of China during the last half century using  
14 historical data, *Water Resources Research*, 40, 308-322, 2004.

15 Yang, D., Sun, F., Liu, Z., Cong, Z., and Lei, Z.: Interpreting the complementary relationship  
16 in non-humid environments based on the Budyko and Penman hypotheses, *Geophysical*  
17 *Research Letters*, 33, 122-140, 2006.

18 Yang, H., Yang, D., Lei, Z., and Sun, F.: New analytical derivation of the mean annual  
19 water - energy balance equation, *Water Resources Research*, 44, 893-897, 2008.

20 Yang, H., and Yang, D.: Derivation of climate elasticity of runoff to assess the effects of  
21 climate change on annual runoff, *Water Resources Research*, 47, 197-203, 2011.

22 Yang, H., Qi, J., Xu, X., Yang, D., and Lv, H.: The regional variation in climate elasticity and  
23 climate contribution to runoff across China, *Journal of Hydrology*, 517, 607–616, 2014a.

24 Yang, H., Yang, D., and Hu, Q.: An error analysis of the Budyko hypothesis for assessing the  
25 contribution of climate change to runoff, *Water Resources Research*, 50(12), 9620-9629,  
26 2014b.

27 Yang, H., Yang, D., Hu, Q. and lv, H.: Spatial variability of the trends in climatic variables  
28 across China during 1961-2010, *Theoretical and Applied Climatology*, 120,773-783, 2015.

29 Zhao, C., Tie, X. and Lin, Y.: Apossible positive feedback of reduction of precipitation and  
30 increase in aerosols over eastern central China, *Geophys Res Lett*, 33, L11814, 2006.

- 1 Zheng, H., Lu Zhang, Ruirui Zhu, Changming Liu, Yoshinobu Sato, and Fukushima, Y.:
- 2 Responses of streamflow to climate and land surface change in the headwaters of the Yellow
- 3 River Basin, Water Resources Research, 45, <http://dx.doi.org/10.1029/2007WR006665>., 2009.



1 Table 1. Principal parameters of the Penman equation

Symbol	Unit	Value	Physical meaning
$\Delta$	kPa °C <sup>-1</sup>	-	slope of the saturated vapor pressure versus air temperature curve
$R_n$	MJ m <sup>-2</sup> d <sup>-1</sup>	-	net radiation
$G$	MJ m <sup>-2</sup> d <sup>-1</sup>	-	soil heat flux
$\gamma$	kPa °C <sup>-1</sup>	-	psychrometric constant
$\lambda$	MJ kg <sup>-1</sup>	2.45	latent heat of vaporization
$e_s$	kPa	-	saturated vapor pressure
$RH$	%	-	relative humidity
$U_2$	m s <sup>-1</sup>	-	wind speed at a height of 2m

2  
3  
4  
5  
6  
7  
8  
9  
10  
11  
12  
13  
14  
15

1 Table 2. Principal parameters of Eq. (12)

Symbol	Unit	Value	Physical meaning
$\alpha_s$	dimensionless	-	albedo or the canopy reflection coefficient
$R_s$	$\text{MJ m}^{-2} \text{ day}^{-1}$	-	solar radiation
$\sigma$	$\text{MJ K}^{-4} \text{ m}^{-2} \text{ day}^{-1}$	$4.903 \times 10^{-9}$	Stefan–Boltzmann constant
$T_{\max}$	$^{\circ}\text{C}$	-	daily maximum air temperature
$T_{\min}$	$^{\circ}\text{C}$	-	daily minimum air temperature
$n$	hour	-	daily actual sunshine duration
$N$	hour	-	daily maximum possible duration of sunshine
$RH$	%	-	daily relative humidity

2  
3  
4  
5  
6  
7  
8  
9  
10  
11  
12  
13  
14  
15  
16

1 Table 3. Validation of the climate elasticity method

Catchments	Upper Bijiang River basin	Upper Luan River basin	Lower Luan River basin	Upper Hanjiang River basin
Study period	1956-2000	1956-2005	1956-2005	1970-2000
$\bar{P}$	495.2	402.4	512.4	850.0
$\bar{E}_0$	1056.9	1257.4	1207.5	1178.0
$\bar{R}_0$	243.4	34	92.6	352
$\Delta P / \bar{P}$	3.9%	-9.8%	1.8%	-11.3%
$\Delta E_0 / \bar{E}_0$	-3.7%	-6.2%	-8.0%	3.0%
$\Delta R$	20.5	-10.1	-29.1	-97.0
$(\Delta R / R)_O$	8.4%	-30.8%	-31.4%	-27.6%
$n$	0.7	1.4	1.4	1.0
$\varepsilon_P$	1.39	2.2	2.1	1.6
$\varepsilon_{E_0}$	-0.39	-1.2	-1.1	-0.6
$(\Delta R / R)_M$	-	-14.0%	12.4%	-19.6%
$(\Delta R / R)_E$	6.9%	-21.4%	9.1%	-19.0%

2 \*  $\bar{P}$  is the mean annual precipitation (mm);  $\bar{E}_0$  is mean annual potential evaporation(mm);  $\bar{R}_0$   
 3 is mean annual runoff (mm);  $\Delta P / \bar{P}$  is the percentage of precipitation change (%);  $\Delta E_0 / \bar{E}_0$  is  
 4 the percentage of potential evaporation change;  $\Delta R$  is the runoff change during the study  
 5 period (mm);  $(\Delta R / \bar{R})_O$  is the percentage of runoff change that was observed;  $n$  is the  
 6 characteristics parameter;  $\varepsilon_P$  and  $\varepsilon_{E_0}$  are the precipitation elasticity and potential evaporation  
 7 elasticity, respectively;  $(\Delta R / R)_M$  and  $(\Delta R / R)_E$  are the percentage of runoff change that was  
 8 estimated by hydrological models and the climate elasticity method, respectively.

1 Table 4. Comparison of the precipitation elasticity between the reference results and the  
2 results from this study

Study Region	Reference	reference results	results from this study
the Luan River basin	Xu et al., 2013	2.6	2.5
the Chao–Bai Rivers basin	Ma et al., 2010	2.4	2.5
the Poyang Lake	Sun et al., 2013	1.4 to 1.7	1.6
the Beijiang River catchment of the Pearl River basin	Wang et al., 2013	1.4	1.4
the Dongjiang River catchment of the Pearl River basin	Jiang et al., 2007	1.0–2.0	1.4

3  
4  
5  
6  
7  
8  
9  
10  
11  
12  
13  
14

1 Table 5. Comparison between the runoff elasticity to climatic factors between the reference  
2 results and the results from this study

Study Region		$\varepsilon_{Rn}$	$\varepsilon_T$	$\varepsilon_{U_2}$	$\varepsilon_{RH}$	Reference
the Futuo River basin	$\varepsilon^*$	-0.79	-0.048	-0.33	0.83	Yang and Yang,2011
	$\varepsilon$	-0.67	-0.047	-0.33	0.80	
the Yellow River basin	$\varepsilon^*$	-0.76	-0.046	-0.59	0.78	Tang et al.,2013
	$\varepsilon$	-1.07 to -0.46	-0.015 to -0.067	-0.55 to -0.1	0.3 to 1.1	
the Hai River basin and the Yellow River basin	$\varepsilon^*$	-1.9 to -0.3	-0.02 to -0.11	-0.8 to -0.1	0.2 to 1.9	Yang and Yang,2011
	$\varepsilon$	-2.0 to 0.3	-0.015 to -0.096	-0.85 to -0.1	0.2 to 2.1	

3 \*  $\varepsilon_{Rn}$ ,  $\varepsilon_T$ ,  $\varepsilon_{U_2}$ , and  $\varepsilon_{RH}$  are the runoff elasticity to net radiation ( $Rn$ ), mean air temperature( $T$ ),  
4 wind speed ( $U$ ), and relative humidity ( $RH$ ), respectively.  $\varepsilon^*$  and  $\varepsilon$  are results from the  
5 references andfrom this study, respectively.

6  
7  
8  
9  
10  
11  
12  
13  
14  
15  
16

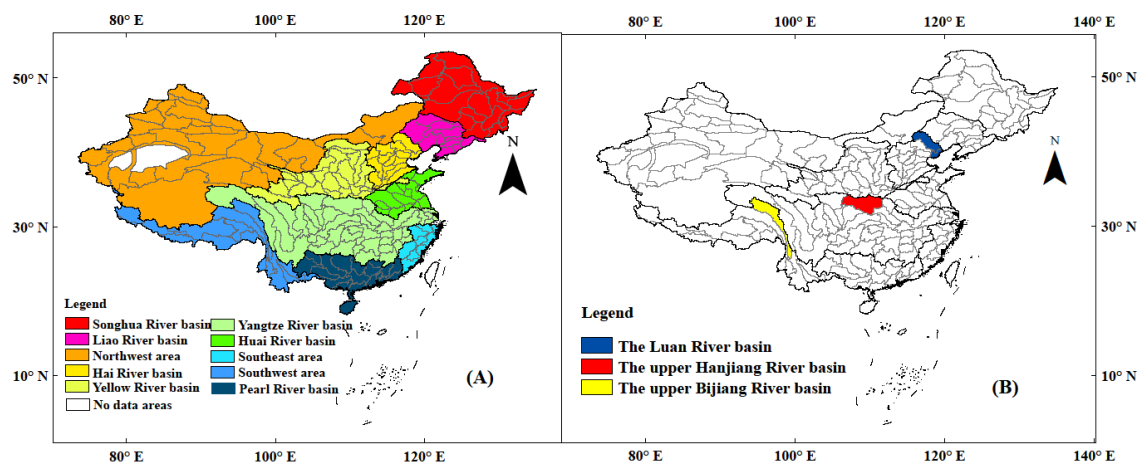


Figure 1. (A) Spatial distribution of third-level river basins in China and (B) three catchments for validation.

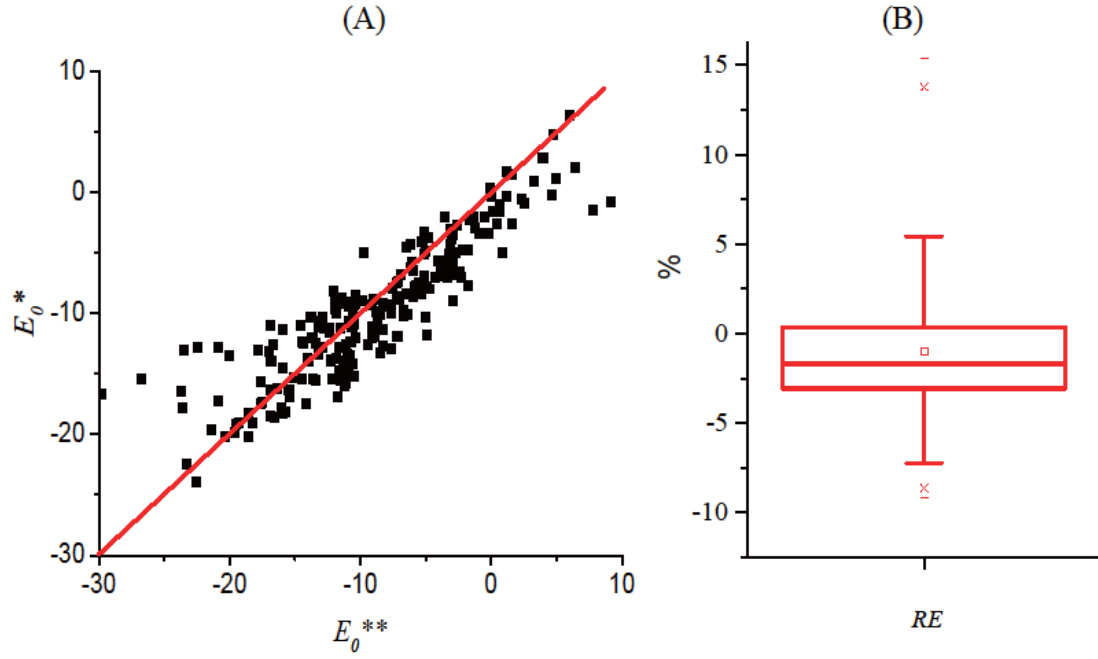


Figure 2. (A) Comparison between the potential evaporation change evaluated by Eq. (9), denoted as  $E_0^*$  (%), and that evaluated by Eq. (17), denoted as  $E_0^{**}$  (%), from 1961–2010, and (B) the relative error ( $RE$ ) (%) caused by the first-order approximation, where  $RE = (E_0^* - E_0^{**}) / E_0^{**}$ ,  $E_0^*$  and  $E_0^{**}$  were the potential evaporation changes evaluated by Eq. (9) and Eq. (17), respectively.

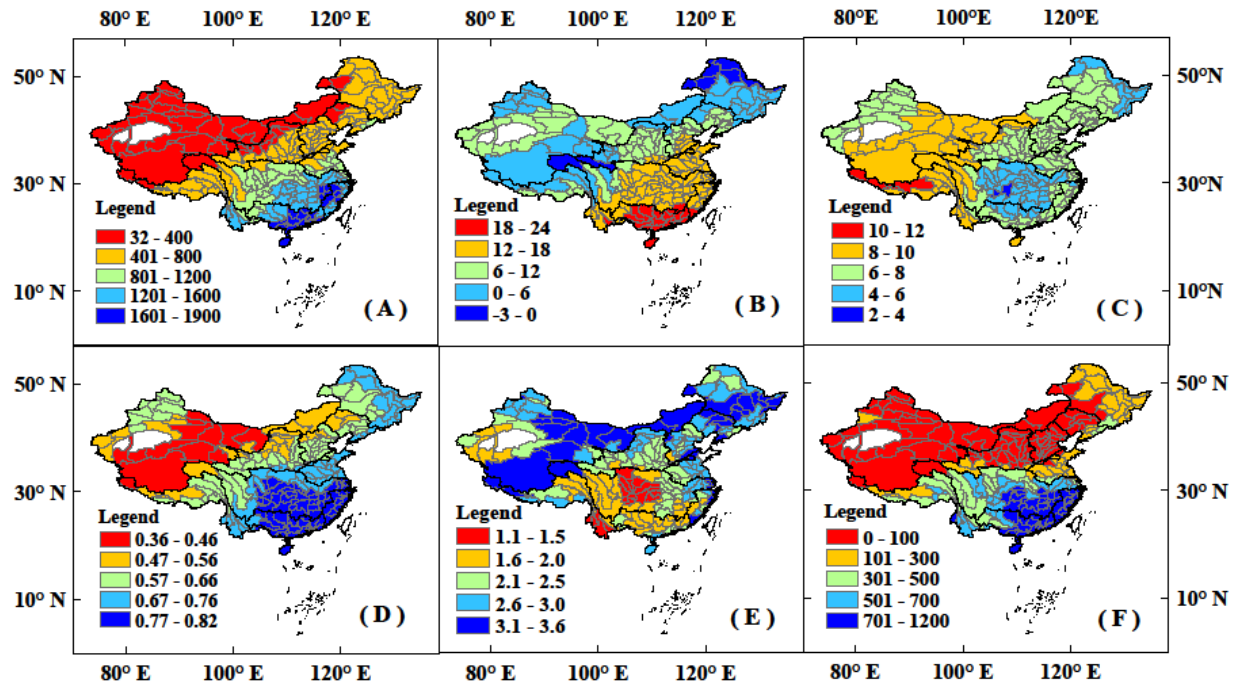


Figure 3. The mean annual (A) precipitation(unit: mm), (B) air temperature (unit: °C), (C) net radiation (unit: MJ m<sup>-2</sup> d<sup>-1</sup>), (D) relative humidity, (E) wind speed at 2m height (unit: m s<sup>-1</sup>), and (F) runoff (unit: mm) in the 207 catchments during 1961-2010.



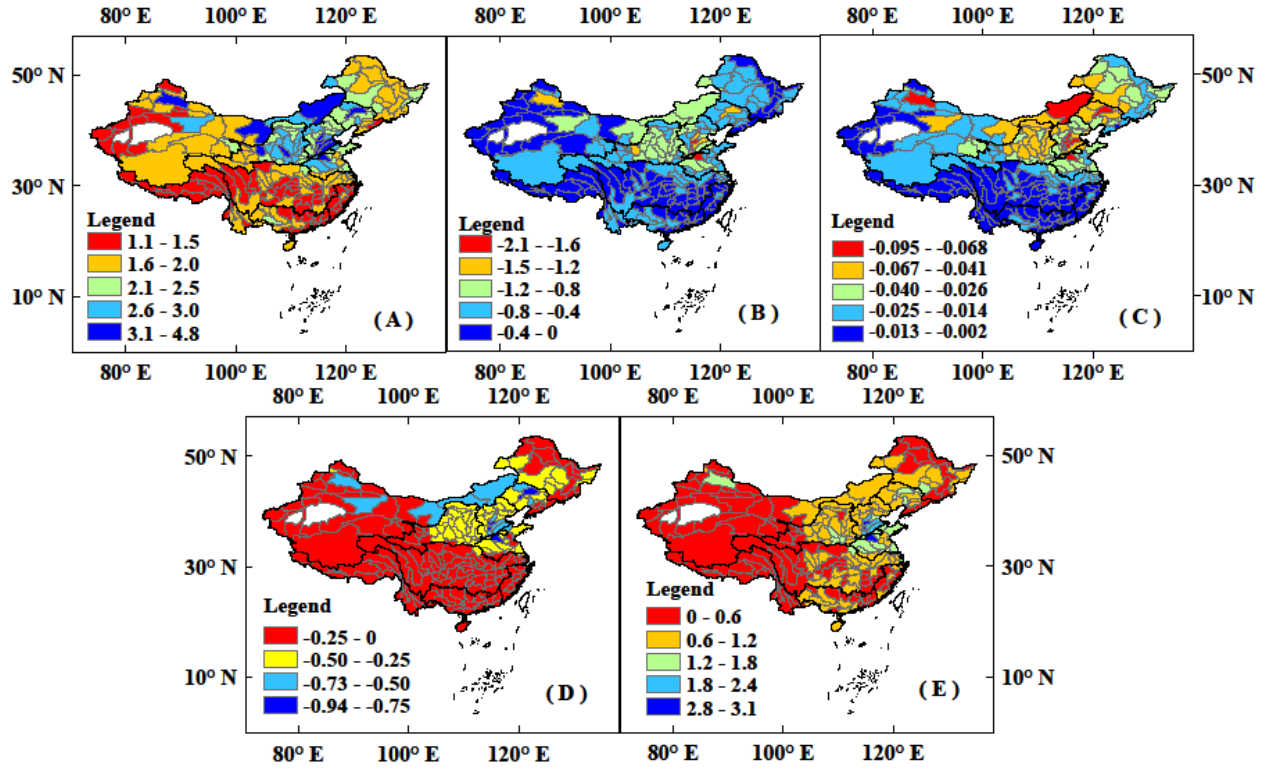
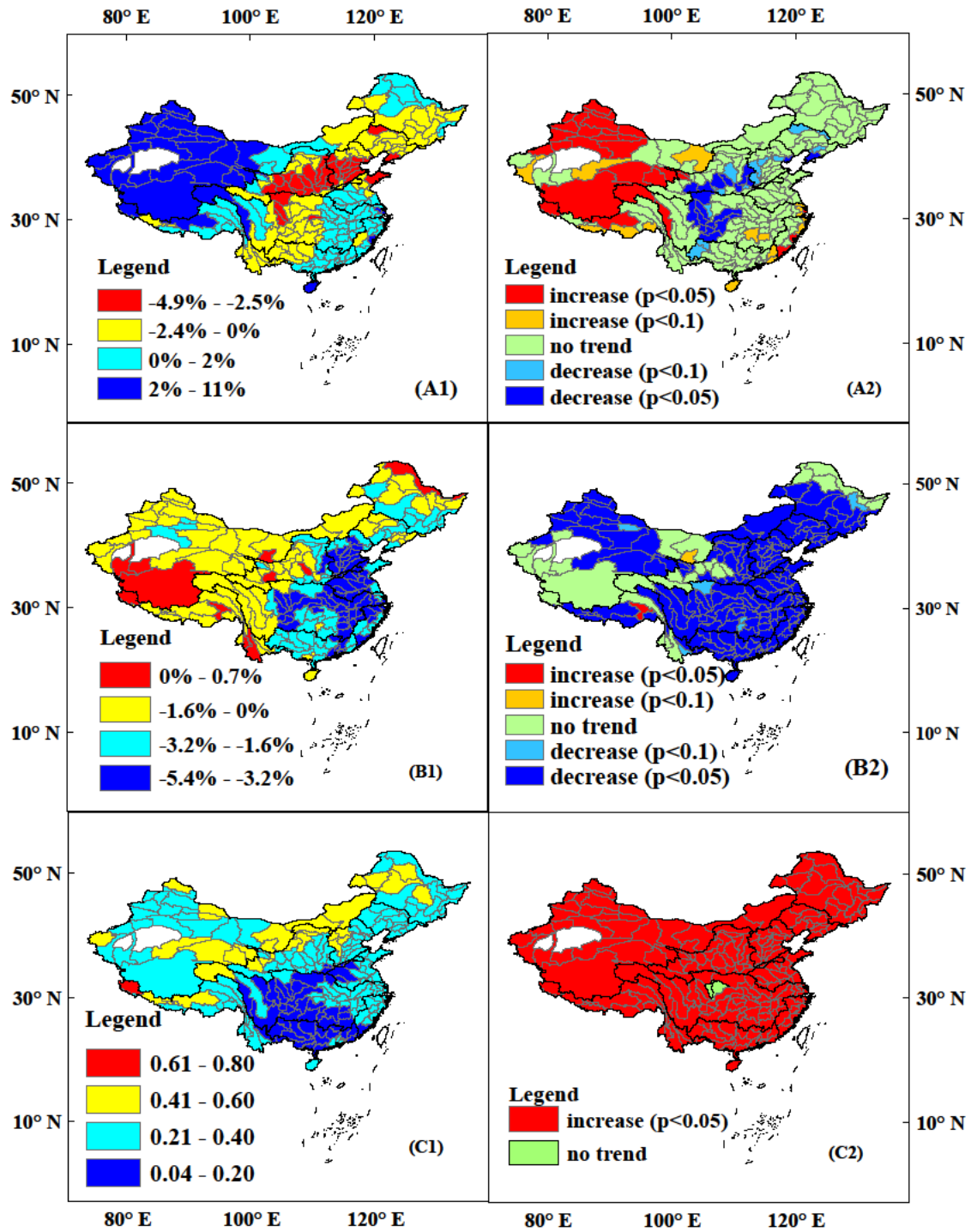


Figure 4. (A) precipitation elasticity  $\varepsilon_P$ , (B) net radiation elasticity  $\varepsilon_{R_n}$ , (C) air temperature elasticity  $\varepsilon_T$  (unit:  $^{\circ}\text{C}$ ), (D) wind speed elasticity  $\varepsilon_{U_2}$ , and (E) relative humidity elasticity  $\varepsilon_{RH}$  of runoff in the 207 catchments.

1

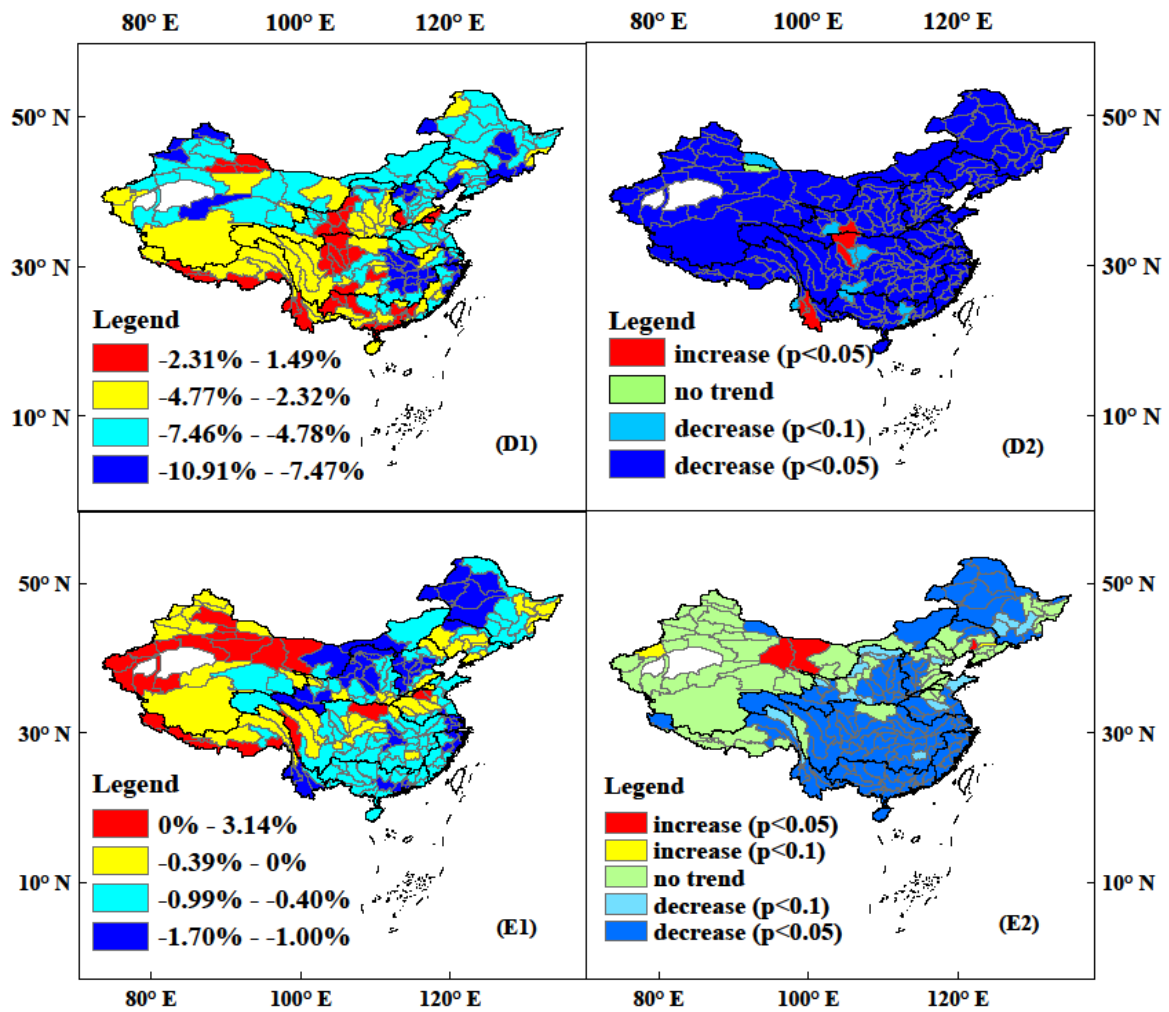


2

3

4

1

2  
3

4 Figure 5. The changing trends for (A1) precipitation (unit: /decade), (B1) net radiation (unit:  
5 /decade), (C1) air temperature (unit: °C/decade), (D1) wind speed (unit: /decade), (E1) relative  
6 humidity (unit: /decade); and the significance of the trends for (A2) precipitation, (B2) net  
7 radiation, (C2) air temperature, (D2) wind speed, (E2) relative humidity to runoff in the 207  
8 catchments from 1961-2010.

9

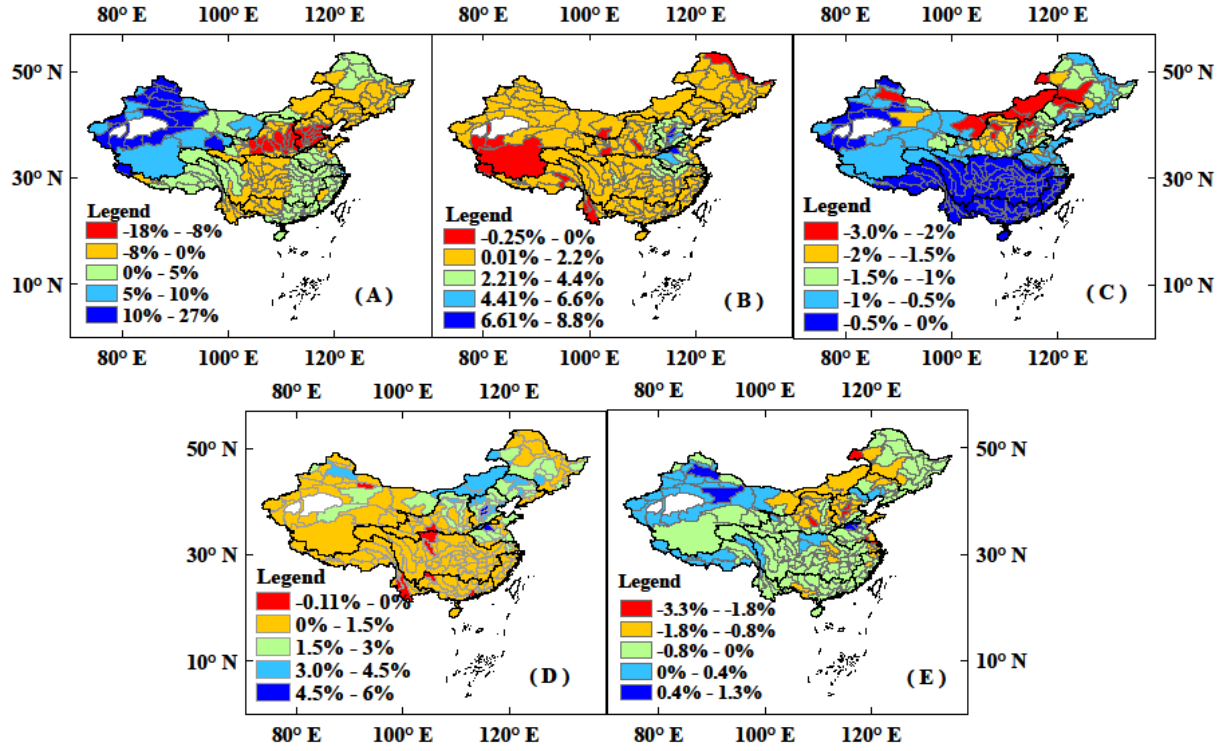


Figure 6. The contribution of (A) precipitation, (B) net radiation, (C) air temperature, (D) wind speed, and (E) relative humidity to runoff change in the 207 catchments from 1961 to 2010 (unit: /decade).

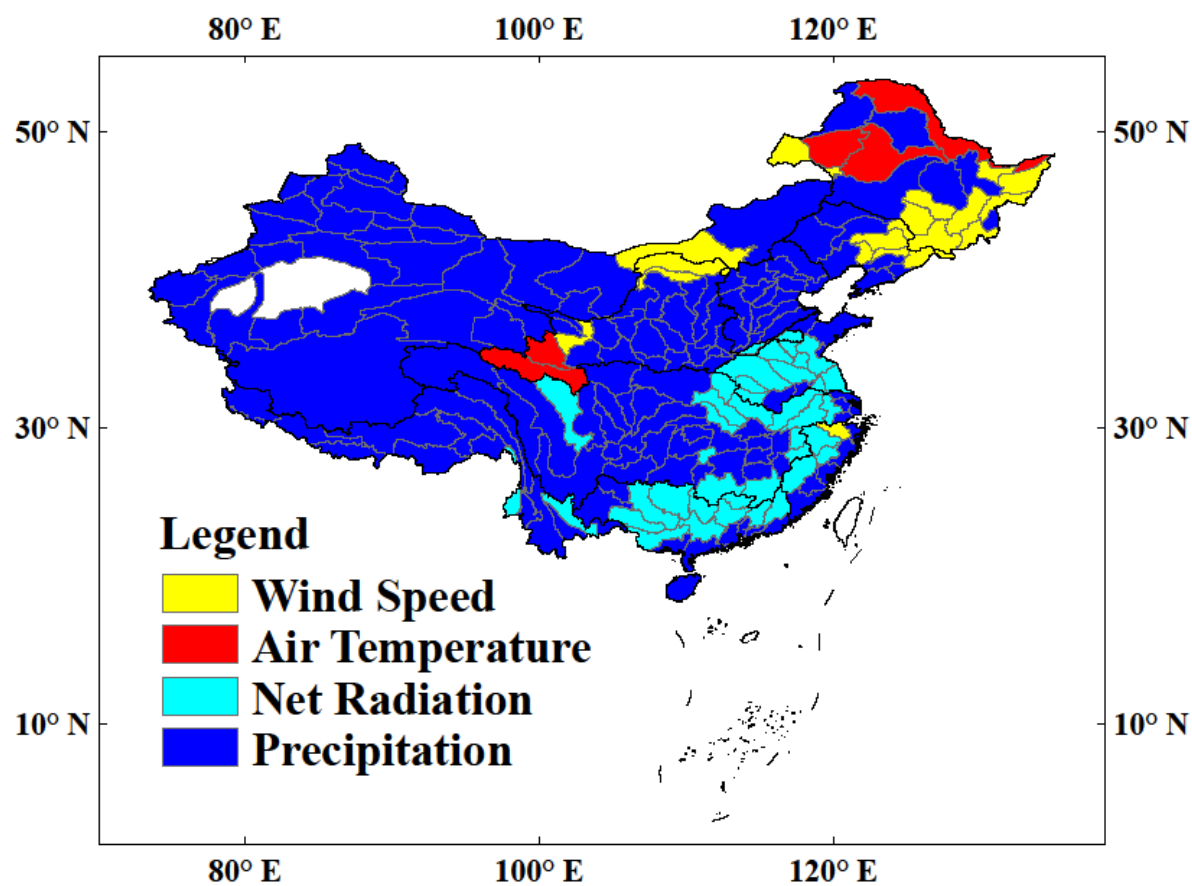


Figure 7. Dominant climatic factors driving annual runoff change in the 207 catchments from 1961 to 2010.

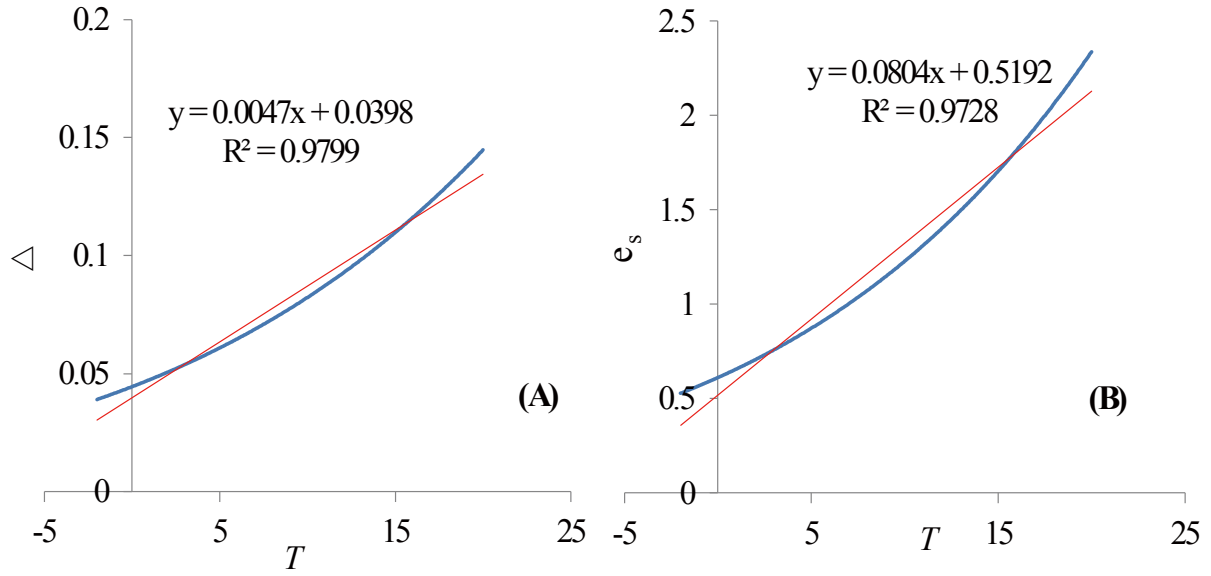


Figure A1. The relationship of (A)  $\Delta$ (kPa/°C) and (B)  $e_s$  (kPa) with temperature  $T$  (°C) change. The blue curves are the relationship of  $\Delta$  and  $e_s$  with  $T$ , respectively; the pink curves show the linear slope of  $\Delta$  and  $e_s$  with  $T$  ( $T$  ranging from  $-2$  °C to  $20$  °C), respectively.

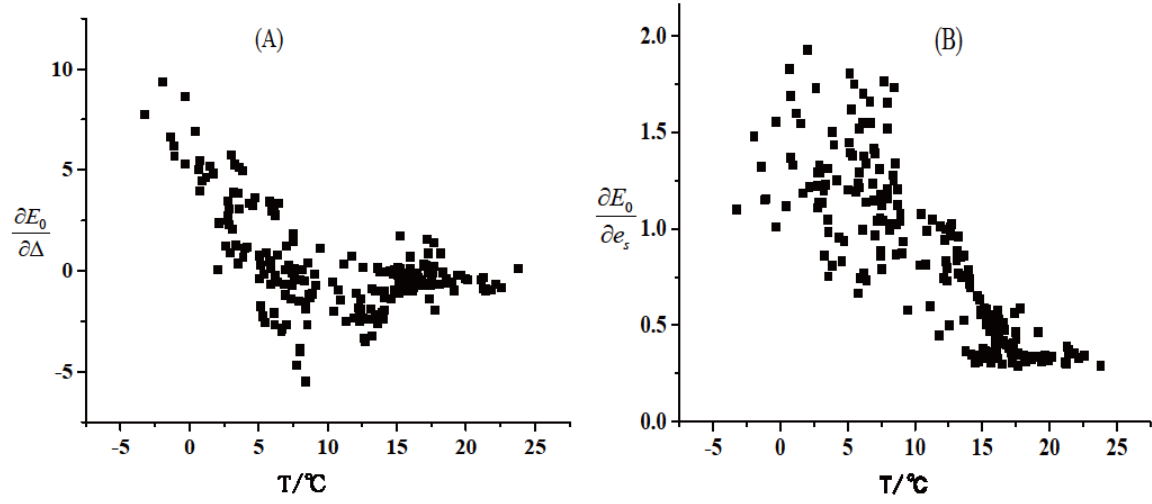


Figure A2. The relationship of (A)  $\frac{\partial E_0}{\partial \Delta}$  and (B)  $\frac{\partial E_0}{\partial e_s}$  with  $T$ , respectively, in the 207 basins of China.

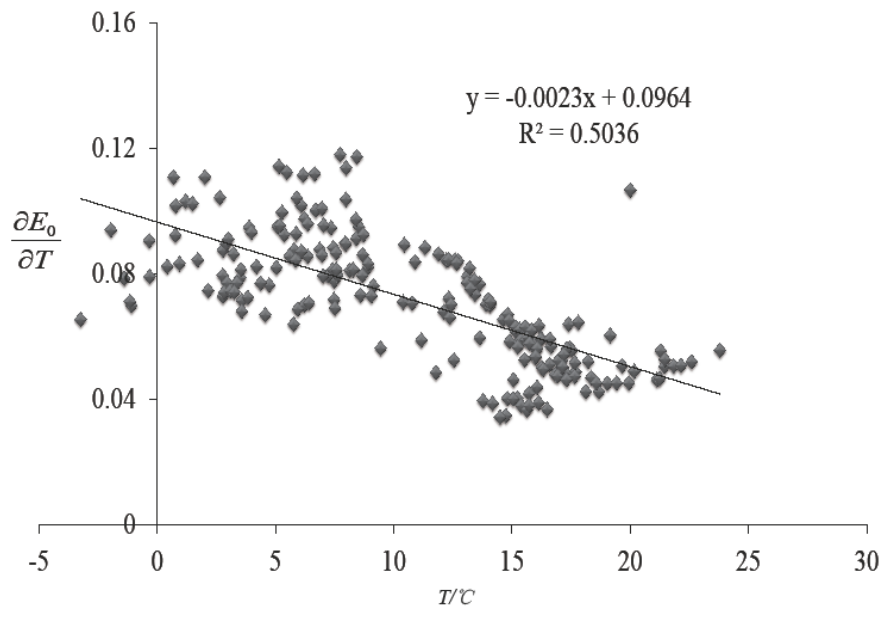


Figure A3. The relationship between  $\frac{\partial E_0}{\partial T}$  and  $T$  in the 207 basins of China.